Petroleum Science 22 (2025) 4381–4393

Contents lists available at ScienceDirect

Petroleum Science

journal homepage: www.keaipublishing.com/en/journals/petroleum-science

Original Paper

Analysis on adsorption capacity of coal, gas content and methane carbon isotope characteristics in coal: A case study from Southwestern Qinshui Basin, China

Ya Meng [a,b,*], Bin Zhang [a,b], Feng-Peng Lai [a,b]

[a] School of Energy Resources, China University of Geosciences (Beijing), Beijing, 100083, PR China
[b] Beijing Key Laboratory of Geology Evaluation and Development of Unconventional Natural Gas, China University of Geosciences (Beijing), Beijing 100083, PR China

ARTICLE INFO

Article history:
Received 28 June 2024
Received in revised form
9 April 2025
Accepted 5 August 2025
Available online 8 August 2025

Edited by Xi Zhang and Jie Hao

Keywords:
Coalbed methane
Langmuir volume
Langmuir pressure
Gas content
Carbon isotope

ABSTRACT

The methane adsorption capacity, gas content, and carbon isotope characteristics of coal are crucial parameters that determine the productivity of coalbed methane (CBM) wells and their development potential. In this paper, test analyses of methane adsorption, gas content and carbon isotope of methane were carried out using 89 samples from the No.3 coal seam in the southwestern part of the Qinshui Basin. Their characteristics and correlations were analyzed. A relationship model between methane adsorption, gas content, carbon isotopes, coal metamorphism and material composition were established, and its controlling mechanism was investigated. The results indicate that the distribution patterns of Langmuir volume and Langmuir pressure in No.3 coal seam are mainly determined by the material composition and the thermal evolution level. The methane gas content in coal is mainly affected by the burial depth, microcosmic composition, mineral content, moisture content and ash yield, adsorption capacity and metamorphism of the coal. The methane carbon isotope ($\delta^{13}C_1$) values in the natural desorbed gas from No.3 coal seam range from −26.95% to −57.80‰, with a mean value of −34.53‰. $\delta^{13}C_1$ in coal shows a two-stage variation pattern with increasing in vitrinite reflectance (R^o_{max}). When R^o_{max} is blow 3.0%, $\delta^{13}C_1$ values of methane in coal become progressively heavier with increasing R^o_{max}. When R^o_{max} reaches or exceeds 3.0%, $\delta^{13}C_1$ values exhibit a lightning trend with further increases in R^o_{max}, which is primarily controlled by the carbon isotope fractionation effects during thermal evolution.

1. Introduction

Coalbed methane (CBM) is a self-generating and self-storing unconventional natural gas that mainly occurs by adsorbed state in coal seams. Reasonable utilization and exploration of CBM are crucial for guaranteeing the secure operation of coal mines, boosting the availability of clean energy, diminishing greenhouse gas emissions, and promoting the development of national carbon peak and carbon neutral strategic goals (Meng and Li, 2018). The productivity and development potential of CBM wells are governed by the methane adsorption capacity, gas content, and carbon isotope characteristics in coal. The coal reservoir has strong adsorption, which is a fundamental difference from typical natural gas reservoirs. In addition, the prerequisite for the production of CBM is the transition from the adsorbed state into the free state, which is determined by the unique adsorbed state occurrence characteristics of CBM. This process is called “desorption”, which is the reverse process of adsorption (Ye and Liu, 2008). The adsorption and desorption characteristics of coal are crucial reservoir parameters that determine the gas content of coal seams and the development potential of CBM. As the exploration and development of CBM continue to advance, surface development has gradually expanded from medium-shallow to deeper depths. Consequently, the understanding of the storage conditions of coal reservoirs required for CBM development has also increased.

* Corresponding author.
E-mail address: mengya@cugb.edu.cn (Y. Meng).
Peer review under the responsibility of China University of Petroleum (Beijing).

https://doi.org/10.1016/j.petsci.2025.08.010

Therefore, conducting research on the adsorption properties of coal, the methane content in coal, and its carbon isotopic characteristics holds significant theoretical and practical importance for the evaluation of CBM resources, the design of development plans, and the prediction of CBM well productivity in the Qinshui Basin (L.T. Cao et al., 2019; Zhang et al., 2019, 2025; Zhou et al., 2020; Tao et al., 2021; Liu et al., 2022; Lin et al., 2023; Li et al., 2024).

In the 1930s, the adsorption and desorption mechanisms of CBM were analyzed by researchers. At that time, methane adsorption properties in coal were studied mainly using Langmuir monolayer adsorption theory and the multilayer adsorption model (Meng et al., 2016; Xu et al., 2021). In addition, research on CBM adsorption/desorption experiments, related models and its control mechanisms and influencing factors were carried out (Su et al., 2005; Mastalerz et al., 2008; Zhang et al., 2009; Lin et al., 2019; Pan et al., 2019). The adsorption/desorption capacities of CBM and its affecting parameters were investigated using isothermal adsorption experiments. Besides, the effects of coal rank, maceral composition, pore structure, coal texture, temperature, pressure and moisture content of coal were revealed on the gas adsorption/desorption performance. At present, the main models for gas adsorption/desorption in coal include Langmuir isothermal adsorption model and its extended versions, the BET multilayer adsorption model and the adsorption potential theory model (Faiz et al., 1992; Mastalerz et al., 2004, 2008; Ma et al., 2011; Skoczylas et al., 2014; Saghafi, 2017), which can reveal the control mechanism of gas adsorption capacity in coal. The gas content of a coal seam refers to the volume of gas contained per unit mass of coal. Besides, gas content of coal seam and its enrichment/accumulation are mainly determined by the conditions of gas generation, storage and preservation. All the factors affecting the mentioned conditions also influence the distribution of gas content in coal seams. The factors include tectonic setting, lithology of the roof and floor strata, coal lithotype and quality, coal rank, burial depth, and hydrogeological conditions. Previous evaluations and predictions of coal seam gas content were conducted using various methods, including: direct measurement of gas content from borehole cores (Saghafi, 2017), coal seam gas gradient analysis (Wang et al., 2002; Esen et al., 2020), geostatistical analysis, Langmuir equation-based prediction models, and geophysical logging-based reservoir parameters prediction methods (Hou et al., 1999; Chen et al., 2005; Li et al., 2005; Meng et al., 2014). These approaches have provided reliable foundations for CBM development planning and productivity assessment.

The methane carbon isotope ($\delta^{13}C_1$) in coal is an effective parameter to reflect the origin and occurrence conditions of CBM. Significant progress and results have been achieved in utilizing methane carbon isotopes for the study of natural gas evolution, gas source identification, and the comparison of source rocks (Martin S., 1980; G.H. Cao et al., 2019; Jiang et al., 2024; Ni et al., 2024). Research indicates that the carbon isotope values of coal-type methane gradually become heavier as the maturity of the source rock increases. There is a logarithmic functional relationship between the carbon isotopes of coal-type methane and the vitrinite reflectance. These findings provide valuable insights for the study of methane carbon isotopes in CBM. Based on the origin of CBM and its geological occurrence conditions, a systematic investigation was conducted on the distribution characteristics and genetic analysis of $\delta^{13}C_1$ in coal. For the research, several explanatory theories and empirical patterns have been proposed. Such as carbon isotope exchange between methane/carbon dioxide, fractionation effects during desorption-diffusion-migration process, thermal maturation-induced fractionation, late-stage biogenic gas generation mechanisms, and hydrodynamic influences. Globally, Methane $\delta^{13}C_1$ in coal exhibit significant variations, with $\delta^{13}C_1$ values ranging from −80‰ to −16.8‰ (Rice, 1993; Meng et al., 2017). Methane $\delta^{13}C_1$ composition in Chinese coal seams is generally lighter, with $\delta^{13}C_1$, values varying significantly across different geological ages and coal ranks (Zhang et al., 2018, 2019). Methane $\delta^{13}C_1$ values in coal show a positive correlation with burial depth, becoming progressively heavier at greater depths. In areas with strong hydrodynamic activity in the coal measures, not only is the gas content relatively lower, but methane also exhibits more pronounced $\delta^{13}C_1$ depletion (Zhang and Tao, 2000; Li et al., 2010, 2021; Bao et al., 2020). The above un derstandings lay the foundation for CBM exploration and development. However, there is still relatively limited data available on the adsorption capacity, $\delta^{13}C_1$ and gas content in developed CBM reservoirs. As a result, the interrelationships between methane adsorption, $\delta^{13}C_1$ and gas content in coal and its controlling mechanisms insufficient understanding, with substantial uncertainty in current CBM exploration approaches. The development of CBM has not yet achieved the anticipated results. Therefore, this study conducted methane adsorption, gas content, and carbon isotope tests on 89 samples from the No.3 coal seam in the southwestern Qinshui Basin. By analyzing the methane adsorption characteristics, gas content, and carbon isotope signatures of the No.3 coal seam, as well as their interrelationships, we established correlation models between methane adsorption capacity, gas content, and carbon isotopes with coal composition and metamorphic degree. Furthermore, the controlling mechanisms were elucidated, providing a theoretical foundation for the development of deep CBM resources in China.

2. Overview of the study area and testing procedures

2.1. Overview of the study area

The study area is situated in the southwestern the Qinshui Basin (Fig. 1(a)), including the Anze-Mabi East–Zhengzhuang block (Fig. 1(b)). Situated in the southeastern part of Shanxi Province, the terrain is complex, mostly hills and mountains. The area is a Late Paleozoic Carboniferous-Permian paralic coal-bearing strata (Fig. 1(c)). The main coal-bearing strata consist of the No.3 coal seam in the Lower Permian Shanxi Formation and the No. 15 coal seam in the Upper Carboniferous Taiyuan Formation. The thickness of the No.3 coal seam in the Shanxi Group is 2.4–7.5 m, which is the main target layer in this region. The research area is primarily the synclinorium structure of the Qinshui Basin, which spreads in the NNE (north-northeast) direction. The northern study area (Anze-Mabi East block) exhibits an overall syncline structure, with uplifted eastern and western flanks and a central depression, trending NNE. The structure of the western flank is relatively simple tectonics, characterized by a southeast-dipping monocline. The block contains small-scale faults with limited extension, predominantly trending NNE. Fold structures are well-developed throughout the region. The southern study area (Zhengzhuang Block) features an overall structural pattern with lower elevation in the north and higher in the south, forming a northwest-dipping slope. The strata exhibit wide-spreading attitudes and gentle, with dip angles generally ranging from 3°–7°, with an average of 4°. In the southeast, two faults with throws of 100–580 m are developed, which dominate the structural framework of the area and have generated a series of NE-trending anticlines and synclines arranged in alternating patterns. The internal structure appears relatively complex, with abundant minor faults (Fig. 1(b)). As the burial depth is controlled by the structure, the No.3 coal seam in the northern and central parts of the research area is shallower western section and deeper eastern section, with burial depths varying from 400 to 1550 m. Similarly, coal seam depth is generally

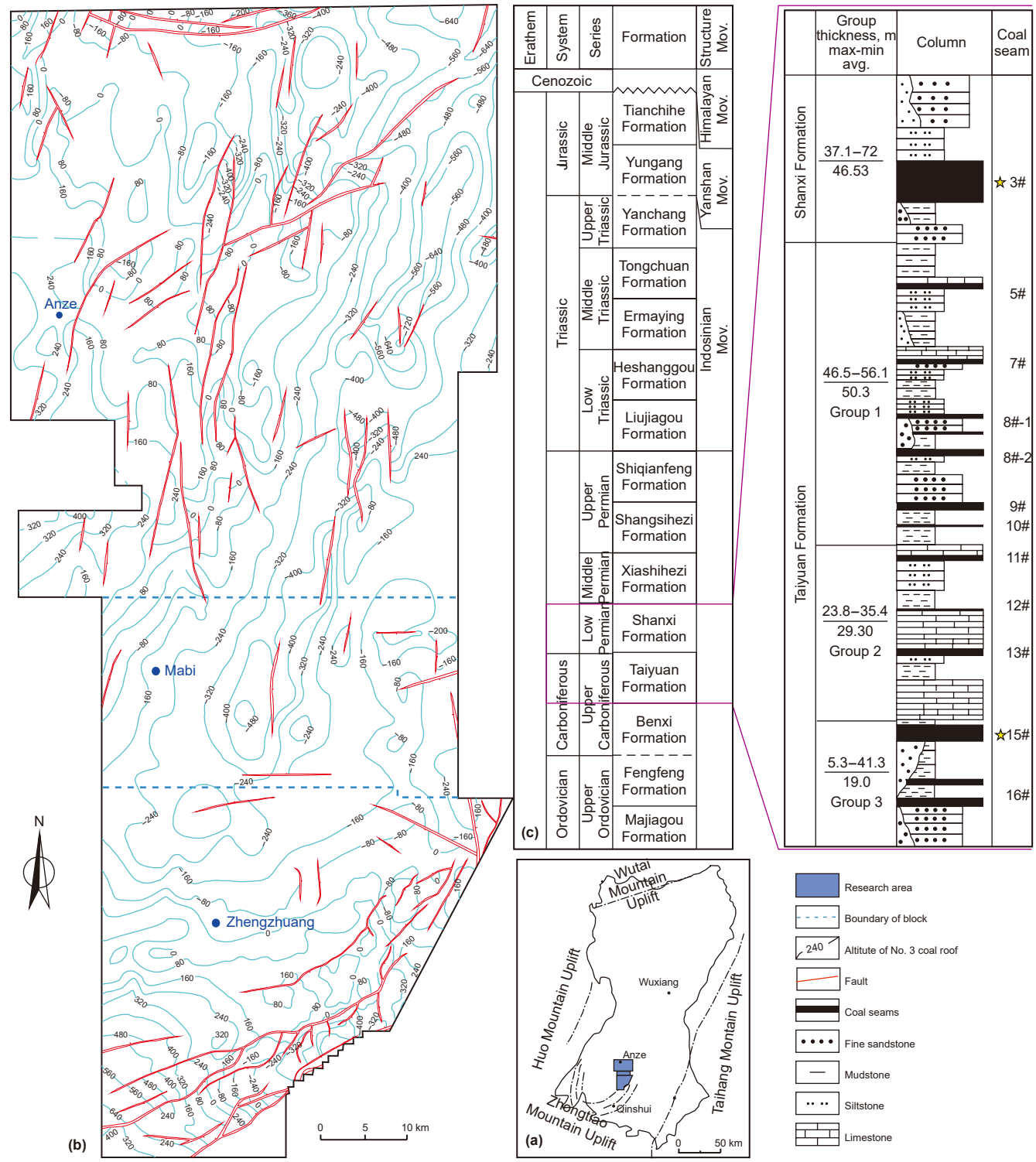

Fig. 1. Contour map of No.3 coal seam floor elevation and comprehensive stratigraphic column in the study area. **(a)** The location of the study area in Qinshui Basin. **(b)** Contour map of No.3 coal seam floor elevation. **(c)** Stratigraphic column of study area.

between 500 and 1200 m in the southern portion of the research area.

2.2. Test sample and procedures

Isothermal adsorption experiments, gas content and $\delta^{13}C_1$ testing of methane in coal were determined for 89 samples from the No.3 coal seam in the research area. The vitrinite reflectance (R^o_{max}) of the coal samples is 1.77%–4.26%, with a mean value of 3.38%. There are three varieties of coal: anthracite, meager coal and lean coal. The macroscopic lithotypes are primarily semi-bright coal and bright coal. The structure mainly consists of primary structural coal. Table 1 shows the analysis results of the basic parameters for the samples.

(1) Methane isothermal adsorption experiment in coal

Table 1
Results of vitrinite reflectance, proximate analysis and coal maceral.

Samples value	R^o_{max}, %	Proximate analysis, %				Coal maceral, %			
		M_{ad}, %	A_{ad}, %	V_{ad}, %	FC_{ad}, %	Vitrinite	Inertinite	Exinite	Mineral
Minimum	1.77	0.69	8.24	5.44	46.92	50.96	7.07	0	2.60
Maximum	4.26	2.45	34.62	18.29	83.20	89.73	44.40	0.55	20.48
Average	3.38	1.31	14.75	8.41	75.53	66.59	26.98	0.01	6.42

The ISO-300 adsorption isotherm device, made by Terra Tek, USA, was used to conduct the isothermal adsorption experiment. The pressure measurement range of this device is 0–70 MPa and the temperature is below 150 °C and the adsorbate is methane gas with a purity of 99.99%. The experiment strictly adhered to the "High-Pressure Isothermal Adsorption Test Method for Coal" (GB/T19560-2008) The coal samples were pulverized and selected with a particle size of 0.2–0.25 mm (equivalent to 60–80 mesh) and a weight of 100–120 g for the isothermal adsorption experiments. Industrial analysis was first performed on the coal samples to determine their ash, moisture, fixed carbon content, and volatile matter before the isothermal adsorption experiment. Setting the system temperature (reservoir temperature) and ensuring that the adsorption equilibrium duration was not shorter than 12 h were two key factors for the whole experiment to meet the standard. In addition, the coal samples were treated with equilibrium moisture before the isothermal adsorption experiments. In the study area, the burial depth of the No.3 coal seam in the Shanxi Formation ranges from 500 to 1500 m, averaging 1000 m; the temperature of the coal reservoir varies between 20 and 40 °C, with an average of 30 °C; and the pressure within the coal reservoir spans from 4.0 to 12 MPa, with an average of 8 MPa. Considering the storage conditions of the coal reservoir in the study area, experimental temperatures were set at 30 °C, and experimental pressures ranged from 0 to 8 MPa.

(2) Methane content test in coal

The measurement of methane content in coal was conducted in accordance with the Chinese National standard of "Methods for Determining Coalbed Methane Content" (GB/T 19559–2021), which is consistent with the US Bureau of Mines method used internationally. The wireline coring technology is often used to determine CBM content. It is required that core retrieval time does not exceed 2 min per 100 m of well depth Upon reaching the surface, cores are immediately sealed in desorption canisters. The desorption process simulates reservoir temperature using a constant-temperature device, with on-site desorption conducted for a total of 8 h. The sample is then sent to the laboratory for continued natural desorption until the average daily desorption volume over 7 consecutive days does not exceed 10 cm^3, at which point the process may be concluded. After samples were crushed, coal samples with a particle size of 2–3 cm were selected and weighed 300–500 g, and loaded into a ball mill tank for residual gas determination. The coal sample is ground for 2–4 h, and after restoring the reservoir temperature, the gas volume is measured. The gas content of coal seam consists of three components: lots gas, desorbed gas, and residual gas. Lost gas is natural gas that escapes from the moment the drill bit penetrates the coal seam until the coal sample is placed in the desorption canister. This portion of gas cannot be measured directly and is usually inferred from the desorption data for the previous 2 h. Desorbed gas is the volume of CBM released under normal atmospheric pressure and reservoir temperature when the coal sample is placed in the desorption canister. The desorption process is considered complete when the average desorption gas content is less than 10 mL/d over a week, or the average desorption content per gram of sample is less than 0.05 mL/d over the same period. In addition, the residual CBM in coal after natural desorption in the previous stage is known as residual gas. Usually, steel balls are placed in a coal sample canister after desorption, which is then sealed and ball-milled for 2 h. The residual gas volume is then determined following the same procedure as the previous stage.

(3) Carbon isotope test of methane in coal

The analyzed samples were collected from the desorbed gas of No.3 coal seam in the Anze, Mabi, and Zhengzhuang Blocks located in the southwestern Qinshui Basin, Shanxi Province. During the drilling of CBM wells wireline coring tools were used to quickly retrieve coal cores, which were then immediately placed into desorption canisters. After 8 h of on-site desorption, laboratory desorption experiments were conducted on the coal seam samples in the canisters. A constant temperature water bath heating method was used to keep the canister temperature close to the reservoir temperature. The timing for gas sample collection is determined when a substantial volume of gas has desorbed, utilizing the liquid displacement method to procure gas samples. The CBM carbon isotope samples are specifically taken from the desorbed gas collected after 24 h of sealing.

The methane carbon isotope analysis was carried out using a MAT253 stable isotope ratio mass spectrometer manufactured by Thermo Fisher Scientific, with an analytical precision of ±0.2‰ (PDB). The experiment was conducted in accordance with SY/T 5238–2019 "Analytical methods for carbon and oxygen isotope in organic matter and carbonate rocks".

3. Analysis and discussion

3.1. Methane adsorption capacity and influencing factors in coal

Methane adsorption in coal belongs to monomolecular layer adsorption, and its adsorption/desorption law conforms to the Langmuir equation, which can be expressed as follows:

$$V = V_L \times P/(P_L + P) \quad (1)$$

where V is the adsorption volume, m^3/t; P is the pressure, MPa; V_L and P_L are the Langmuir volume, m^3/t and the Langmuir pressure, MPa, respectively.

V_L determines the maximal adsorption capacity of the coal. P_L is a significant factor that affects the adsorption isotherm, which refers to the pressure value when the adsorbed capacity reaches 50% of V_L. The distribution of V_L and P_L in the No.3 coal seam has the following characteristics:

(1) V_L of the air-dry basis (raw coal) for the No.3 coal reservoir generally exhibits an upward trend from northwest to southeast and from north to south. In the Anze and Mabi blocks, the V_L increases from northwest to southeast and is

generally less than 35 m^3/t. V_L contour spreads in a northeast-southwest direction. However, V_L of the Zhengzhuang block increases from north to south and has some local variations. V_L of the block is generally larger than 35–47.10 m^3/t (Fig. 2(a)).

(2) P_L of the No.3 coal reservoir is consistent with V_L distribution. In the Anze and Mabi blocks, north to south and northwest to southeast observe a progressive increase in P_L. P_L is distributed from northeast to southwest and is generally less than 3.0 MPa. However, P_L in the Zhengzhuang block also increases gradually in the north-south and west-east directions, with some local variations (Fig. 2(b)).

(3) V_L and P_L of the No.3 coal reservoir show a positive relationship (Fig. 3). The area with a large V_L corresponds to a

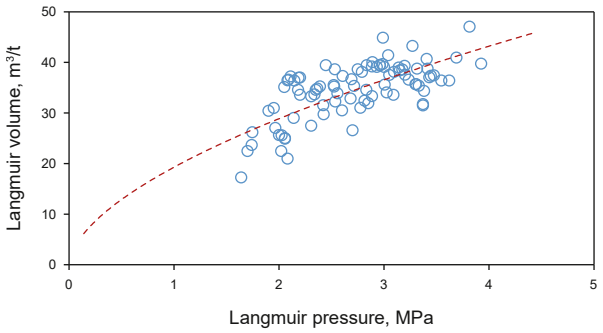

Fig. 3. Relationship between Langmuir volume and Langmuir pressure of air-dried coal samples in the study area.

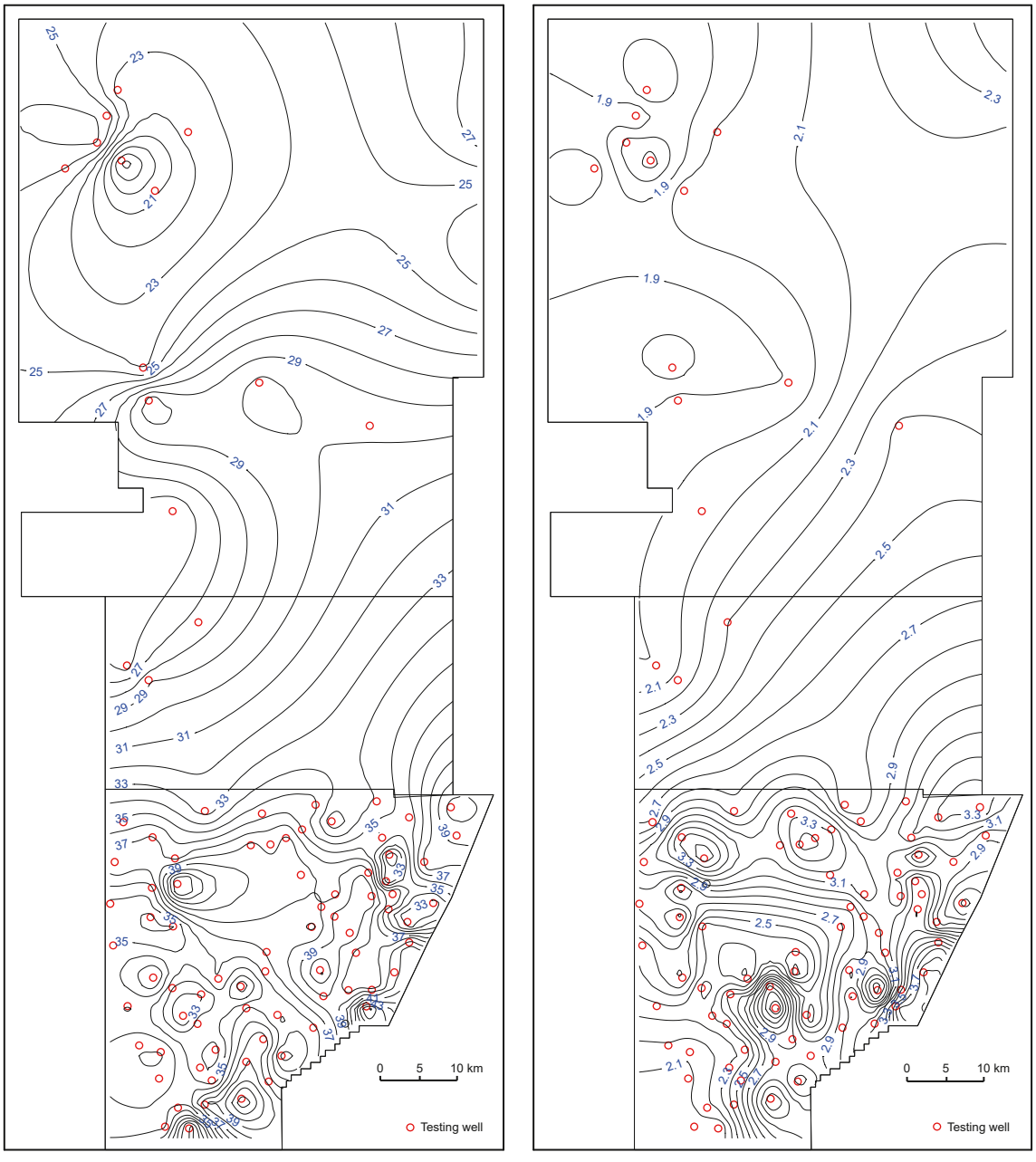

(a) Langmuir volume **(b)** Langmuir pressure

Fig. 2. Distribution of Langmuir volume and Langmuir pressure in No. 3 coal seam in the study area. **(a)** Langmuir volume. **(b)** Langmuir pressure.

higher P_L, which is advantageous for the development of CBM. Due to the differences in coal lithology, coal quality, porosity, pore structure, degree of metamorphism, reservoir pressure, and temperature across the horizontal plane, there are some differences in coal adsorption capacity for the same coal seam.

V_L and P_L distribution characteristics of the No.3 coal seam are mainly determined by the material composition and thermal evolution level of the coal. These characteristics are shown below:

(1) V_L and P_L of air-dried coal samples increase with maceral content and obey a logarithmic function (Fig. 4). In addition, they also decrease with increasing mineral content and obey a negative exponential function (Fig. 5), with the following relationships:

$$V_L = 86.277 \ln(O) - 356.93 \quad (2)$$

$$P_L = 5.315 \ln(O) - 21.398 \quad (3)$$

where O is the maceral content, %. The determination coefficients R^2 of Eq. (2) and Eq. (3) are 0.38 and 0.14, respectively. The total number of statistics is 89.

$$V_L = 42.02e^{-0.032M} \quad (4)$$

$$P_L = 3.11e^{-0.024M} \quad (5)$$

where M is the mineral content in coal, %. The determination coefficients R^2 of Eq. (4) and Eq. (5) are 0.36 and 0.14, respectively. The number of statistics is 89.

(2) V_L and P_L of air-dried coal samples decrease with the increase in moisture content and ash yield in the coal and obey the variation of negative exponential function relationship (Fig. 6), which is shown below:

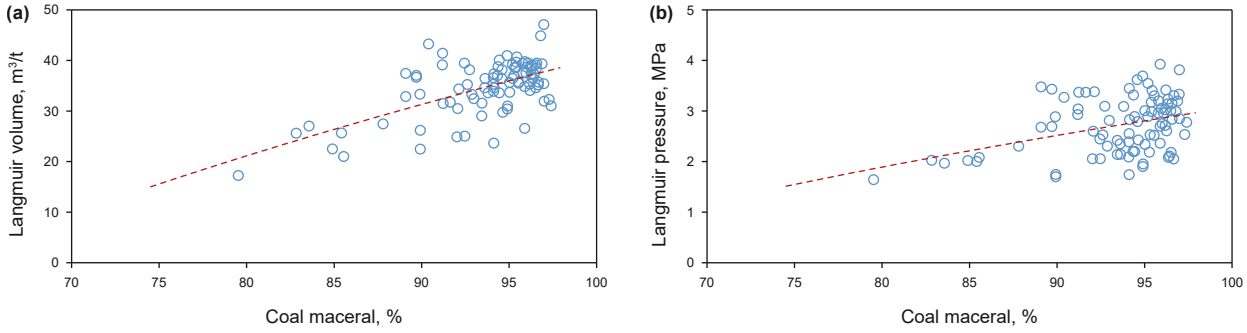

Fig. 4. Relationship between Langmuir volume and Langmuir pressure of air-dried coal samples and coal maceral. **(a)** Langmuir volume. **(b)** Langmuir pressure.

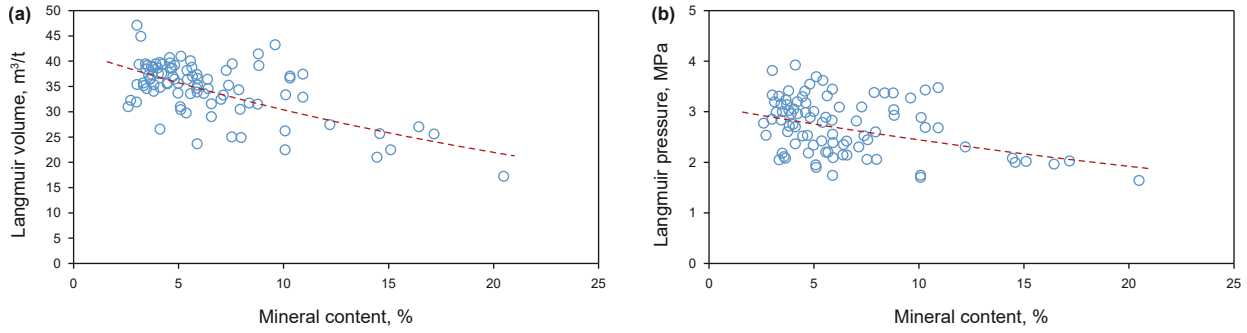

Fig. 5. Relationship between Langmuir volume and Langmuir pressure of air-dried coal samples and mineral content in coal. **(a)** Langmuir volume. **(b)** Langmuir pressure.

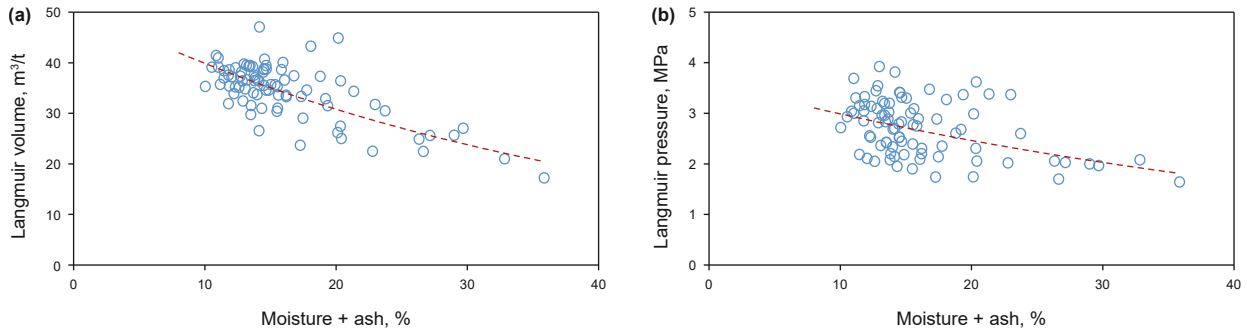

Fig. 6. Relationship between Langmuir volume and Langmuir pressure and moisture + ash for air-dried coal samples. **(a)** Langmuir volume. **(b)** Langmuir pressure.

$$V_L = 51.64e^{-0.026S} \quad (6)$$

$$P_L = 3.63e^{-0.019S} \quad (7)$$

where S is the sum of the moisture content and ash yield in coal, %. The determination coefficients R^2 of Eq. (6) and Eq. (7) are 0.48 and 0.18, respectively. The total number of statistics is 89.

(3) Ash yield and moisture content in coal are correlated with methane adsorption. Methane adsorption in coal decreases with increasing equilibrium water content and ash yield and obeys a logarithmic function relationship (Fig. 7). The relationship is shown below:

$$\Delta V_1 = -3.355\ln(W) + 3.4549 \quad (8)$$

$$\Delta V_2 = -3.951\ln(A) + 4.6088 \quad (9)$$

$$\Delta V_1 = Q_2 - Q_1 \quad (10)$$

$$\Delta V_2 = Q_1 - Q_3 \quad (11)$$

where ΔV_1 is the amount of adsorption reduced by the influence of equilibrium moisture in coal, m^3/t; ΔV_2 is the amount of adsorption reduced by the influence of ash yield in coal, m^3/t; W is the equilibrium moisture content, %; A is the ash yield, %; Q_1, Q_2 and Q_3 are the Langmuir volumes of air-dried, equilibrium moisture, and dry ash-free coal samples, respectively, m^3/t. The determination coefficients R^2 of Eqs. (8) and (9) are 0.30 and 0.42, respectively, and the total number of statistics is 89.

The adsorption capacity of methane in coal is significantly influenced by the moisture content. Both the properties of moisture and gas molecules in coal are similar to the coal structure. There are no covalent bonds between water molecules and coal; Instead, they are adsorbed in coal through weaker van der Waals forces, which indicates that coal physically adsorbs water molecules. Because water is a polar molecule, the presence of polar bonds induces a stronger and tighter bonding forces between the water molecules and the inner surface of the coal pores, as well as between the water molecules. Water molecules are preferentially adsorbed in coal compared to methane, thus occupying some of the adsorption sites that would otherwise be available for gas molecules. Moisture is extremely important in coal. The presence of water decreases the amount of methane adsorbed by the coal. When the moisture content is below the critical moisture content, methane adsorption reduces only if the moisture increases. However, once the critical moisture content is exceeded, gas adsorption is not affected by the additional moisture (Meng and Li, 2018).

(4) Within the range where the vitrinite reflectance (R^o_{max}) is less than 4.0%, the adsorption capacity of coal in the study area exhibits a positive correlation with the distribution of the maximum vitrinite reflectance (R^o_{max}) values (Fig. 8). V_L and P_L of air-dried coal samples increase with vitrinite reflectance, which obeys the changing rule of the logarithmic function:

$$V_L = 20.763\ln(R^o_{max}) + 9.724 \quad (12)$$

$$P_L = 1.646\ln(R^o_{max}) + 0.749 \quad (13)$$

where the determination coefficients R^2 of Eq. (12) and Eq. (13) are 0.65 and 0.40, respectively. The total number of statistics is 89.

The time (d) needed for 63.2% of the gas in coal to desorb is known as the adsorption time of coal. When R^o_{max} is less than 3.0%, the adsorption time for coal declines with the increase of R^o_{max} (Fig. 8), which demonstrates that methane in coal is easy to desorb with increasing R^o_{max}, resulting in a shorter desorption time. When R^o_{max} is greater than or equal to 3.0%, the adsorption time for coal increases with the increase of R^o_{max} (Fig. 9), which shows that

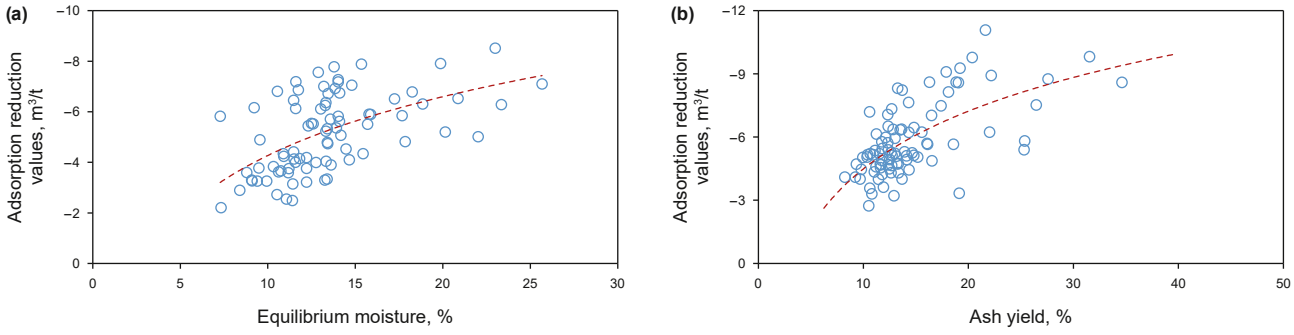

Fig. 7. Relationship between adsorption reduction values and equilibrium moisture and ash yield. **(a)** equilibrium moisture. **(b)** ash yield.

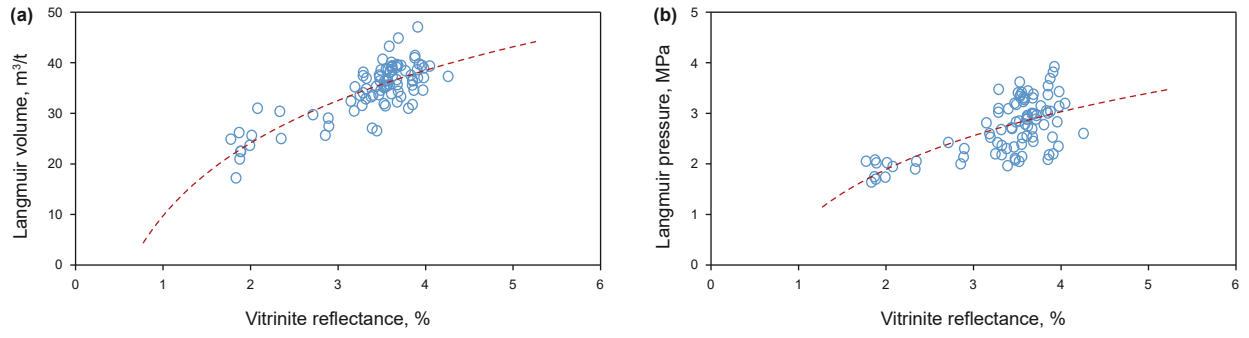

Fig. 8. Relationship between Langmuir volume and Langmuir pressure of air-dried coal samples and vitrinite reflectance. **(a)** Langmuir volume. **(b)** Langmuir pressure.

methane in coal is difficult to desorb with further increasing R^o_{max}, resulting in a longer desorption time.

Based on a comparative analysis of high-rank and low-rank coal samples, Chen and Wang et al. (2008) found that the capacity adsorption of methane shows a three-stage variation pattern with increasing coal rank. In the first stage, when R^o_{max} is below 1.5%, V_L of coal greatly improves with the advancement coalification. In the second stage, when R^o_{max} is 1.5–3.5%, V_L maintains relatively stable and reaches a maximum value. In the third stage, when R^o_{max} is above 3.5%, V_L declines with further coalification. Su et al. (2005) experimentally concluded that the connection between R^o_{max} and V_L showed an inverted U shape curve, which can be divided into four stages. In the first stage, V_L of coal rises rapidly with coalification when R^o_{max} is 0.6%–1.3%. In addition, this stage has the fastest growth rate in the entire evolution process. In the second stage, V_L rises with coalification when R^o_{max} is 1.3%–2.5%. Moreover, compared to the first stage, the rate of this stage is reduced. In the third stage, V_L reaches its maximum value and the rate of change is at its minimum when R^o_{max} reaches 2.5%–4.0%. In the fourth stage, V_L declines rapidly with further coalification when R^o_{max} exceeds 4.0%. The coalification determines the changing rules of coal adsorption capacity. By analyzing the results of isothermal adsorption experiments on different coal rank samples, Wang and Fu (2008) conducted isothermal adsorption tests on 42 coal samples from different regions and discovered that the adsorption properties of coal exhibit a two-stage variation with the progression of metamorphism. The relationship between V_L and vitrinite reflectance shows an inflection point around a R^o_{max} of 4.0%. When the R^o_{max} is less than 4.0%, the V_L of coal increases with the degree of coalification. Conversely, when the R^o_{max} is greater than or equal to 4.0%, the V_L decreases as coalification advances. This pattern of change is governed by the fourth leap transformation in the coalification process.

3.2. Methane content in coal and its affecting factors

The gas content of coal reservoirs is affected by geological structure, lithology of the roof and floor strata, coal petrology and coal quality, coal rank, burial depth, and hydrogeologic conditions. According to the national standard of "Methods for Determining CBM Content" (GB/T 19559–2021), 89 samples from the No.3 coal seam in the southwestern Qinshui Basin were determined for methane content, including the Anze-Mabidong-Zhengzhuang blocks. The result shows the methane content of the No.3 coal seam is 8.28–30.92 m^3/t, averaging 20.17 m^3/t, which conforms to the distribution rule for R^o_{max}. The gas content of coal reservoirs gradually increases from northwest to southeast or south, and it is mainly distributed in the northeast-southwest orientation. In addition, the minimal gas content of the No.3 coal seam is 8.28 m^3/t in the northwestern Anze block. However, in the southern Zhengzhuang block, except at the boundary of the southeast fault, the gas content of No. 3 coal seam is generally above 16 m^3/t and there are some internal variations. Besides, higher gas concentrations (>20 m^3/t) are observed along the NNW-SSE-trending synclinal axis, particularly in the northern Zhengzhuang block, the central Mabi block, and the southeastern Anze block (Fig. 10).

The test results illustrate that the distribution of CBM content in the research region exhibits the following characteristics:

(1) Both the gas content and preservation capacity of CBM increase with the burial depth (Fig. 11). After the End-Triassic, the decrease in CBM may be caused by crustal uplift and erosion. The natural release of CBM is controlled by the burial depth of the coal reservoirs. At shallow depths, CBM

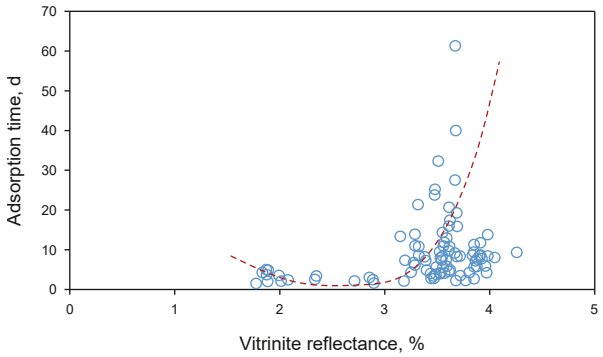

Fig. 9. Relationship between the adsorption time of coal and vitrinite reflectance.

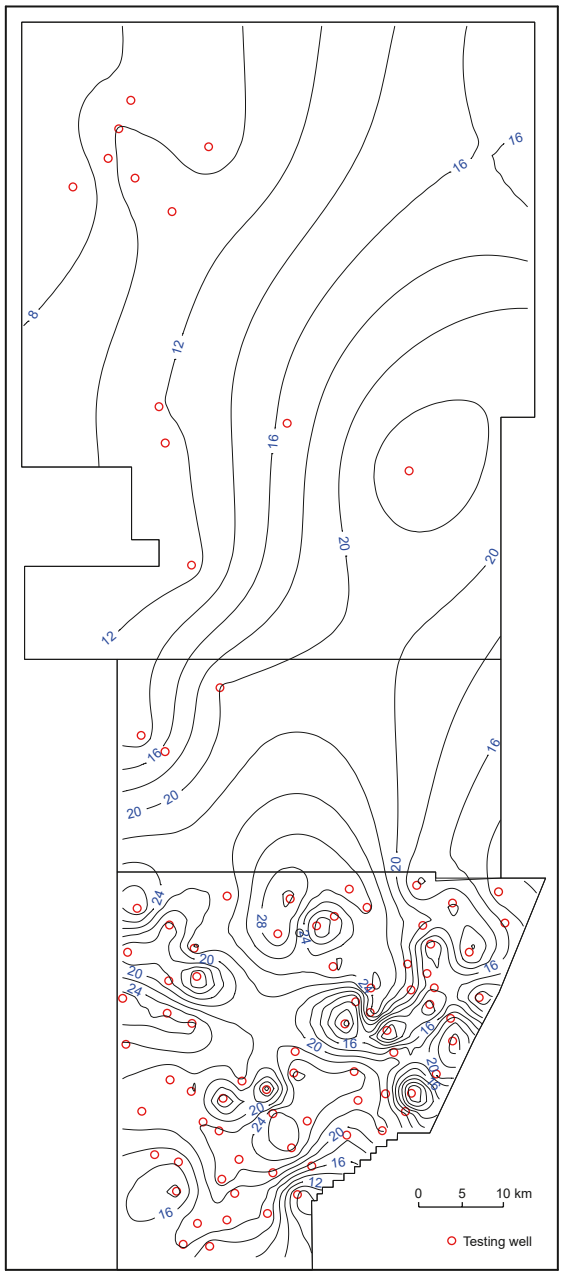

Fig. 10. Contour map of methane gas content of No.3 coal in the study area.

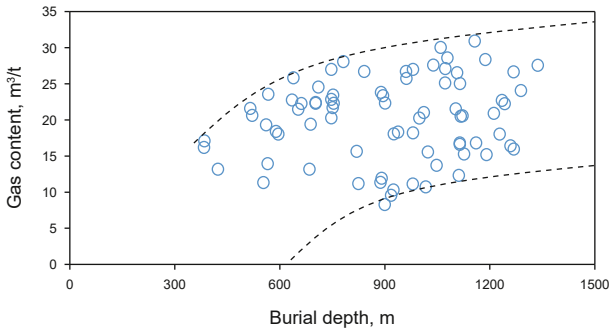

Fig. 11. Relationship between gas content and burial depth of coal reservoir.

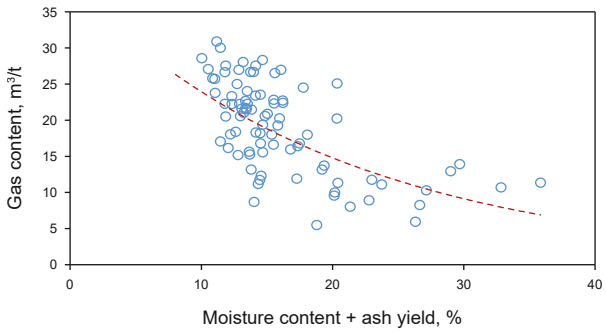

Fig. 13. Relationship between gas content and moisture content + ash yield.

diffuses into the atmosphere along weathering fissures. At the same time, a part of the CBM will be dissolved and carried away due to the flow of groundwater. At significant depths, it is extremely difficult for CBM to diffuse into the atmosphere along weathering fissures (weathering fissures are not developed). Additionally, restricted groundwater flow (or stagnant conditions) minimizes methane loss via aqueous transport (Meng et al., 2017).

(2) The gas content of coal seams increases with maceral content and obeys the logarithmic function relationship (Fig. 12 (a)). Besides, the gas content of the coal seam decreases with increasing mineral content and follows a negative exponential function relationship (Fig. 12(b)). In addition, the gas content decreases with increasing moisture and ash yield in coal, obeying a negative exponential function relationship (Fig. 13). The relationship is as follows:

$$Q = 70.996\ln(O) - 302.19 \tag{14}$$

$$Q = 25.86e^{-0.047M} \tag{15}$$

$$Q = 38.771e^{-0.048S} \tag{16}$$

where Q is gas content in coal, m^3/t; O is the content of maceral, %; M is the mineral content in coal, %; S is the sum of moisture and ash yield in coal, %. The determination coefficients R^2 of Eqs. (14)–(16) are 0.23, 0.23, and 0.43, respectively. The total number of statistics is 89.

(3) Coal metamorphism determines the gas content of coal seams. The gas content of coal seams increases with R^o_{max}, obeying a logarithmic function (Fig. 14). The relationship is as follows:

$$Q = 17.263\ln(R^o_{max}) - 0.5487 \tag{17}$$

where the determination coefficient R^2 is 0.38 and the total number of statistics is 89.

For the No. 3 coal seam of the Shanxi Formation in the study area, the maximum vitrinite reflectance ranges between 1.77% and 4.26%, classifying it as medium to high-rank coal. The CBM primarily exists in an adsorbed state within the coal seam. As the vitrinite reflectance of the coal increases, so does its adsorption capacity, leading to higher methane content in the coal. As illustrated in Fig. 10, the vitrinite reflectance values increase from the shallow to the deep parts of the study area, correspondingly enhancing the coal's adsorption capacity. The methane content in the coal gradually increases from the northwest towards the southeast or south, aligning with the distribution pattern of the maximum vitrinite reflectance in the coal.

(4) The gas content and adsorption capacity of coal are tightly related. The gas content increases with V_L and P_L in coal,

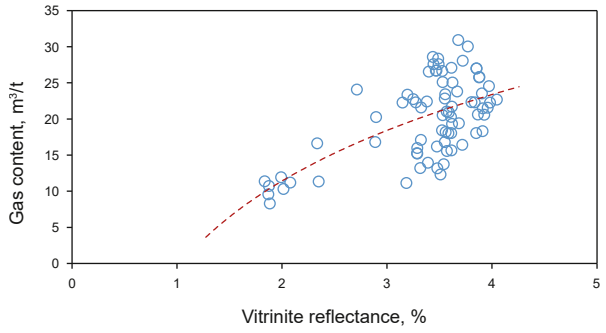

Fig. 14. Relationship between the coal seam gas content and vitrinite reflectance.

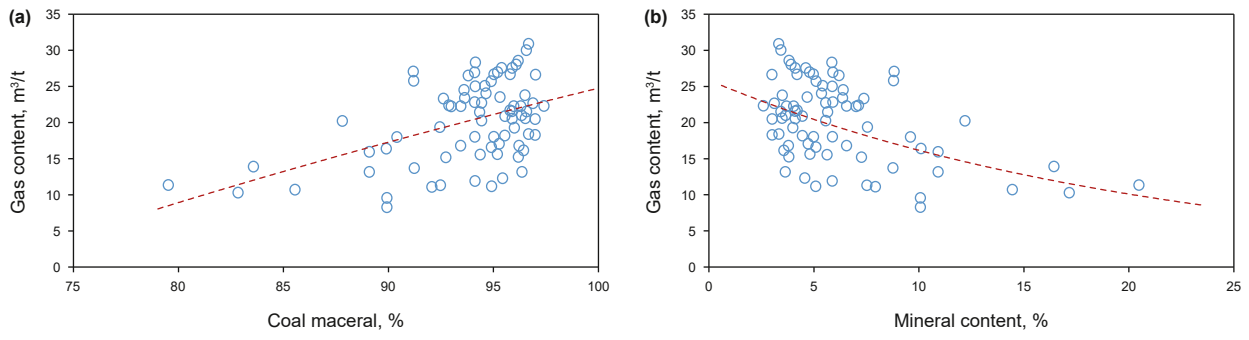

Fig. 12. Relationship between gas content of coal reservoirs and coal maceral and mineral content. **(a)** coal maceral. **(b)** mineral content.

which obeys a power function relationship. (Fig. 15). The relationship is as follows:

$$Q = 0.1632V_L^{0.9762} \quad (18)$$

$$Q = 9.8579P_L^{0.6877} \quad (19)$$

where the determination coefficients R^2 of Eqs. (18) and (19) are 0.20 and 0.17, respectively. The total number of statistics is 89.

3.3. Characterization of carbon isotope in CBM and its control mechanism

The methane $\delta^{13}C_1$ is regarded as one of the significant parameters for the evaluation of CBM resources. The methane $\delta^{13}C_1$ values in CBM range from −78‰ to −13‰. Most of the $\delta^{13}C_1$ values in CBM range from −70‰ to −40‰ (Faiz et al., 1992; Skoczylas et al., 2014). According to the statistics of 89 samples from the No.3 coal seam, the characteristics of $\delta^{13}C_1$ in CBM are as follows:

(1) The composition of No.3 CBM from the Shanxi Formation in this area exhibits relative simplicity, with methane as the main component. The detailed components of CBM are as follows: Methane content is generally 46.83%–98.75%, with an average value of 94.36%; N_2 content is 0.29%–50.85%, with an average value of 4.73%; CO_2 content is 0.19%–3.70%, with an average value of 0.9%. Some samples contain small amounts of heavy hydrocarbons ranging from 0–0.23%, with an average value of 0.01%.

(2) The $\delta^{13}C_1$ values of naturally desorbed gas from the No.3 coal seam range from −26.95‰ to −57.80‰, with an average of −34.53‰. A comparison of No.3 coal seam in this area with the Fanzhuang block in the southern Qinshui Basin shows that the $\delta^{13}C_1$ values in coal are the same. The $\delta^{13}C_1$ values of Fanzhuang block is between −30.30‰ and −48.20‰, with a mean of −35.37‰ for its No.3 coal seam.

(3) The spatial distribution of $\delta^{13}C_1$ values in the No.3 coal seam show the following characteristics: in the northern part, the $\delta^{13}C_1$ values are heavier from northwest to southeast. In the southern part, the $\delta^{13}C_1$ values gradually increase from southeast to northwest. The $\delta^{13}C_1$ values are heavy in the southern Anze block and Mabi block. The carbon isotopes are generally greater than −31‰, with a variation range of −26.95‰ to −31‰, spreading in a north-east direction. However, the $\delta^{13}C_1$ values are lighter in coal from the northern Anze block and Zhengzhuang block. As seen in Fig. 16, the $\delta^{13}C_1$ is generally less than −31‰ and varies from −31‰ to −57.80‰.

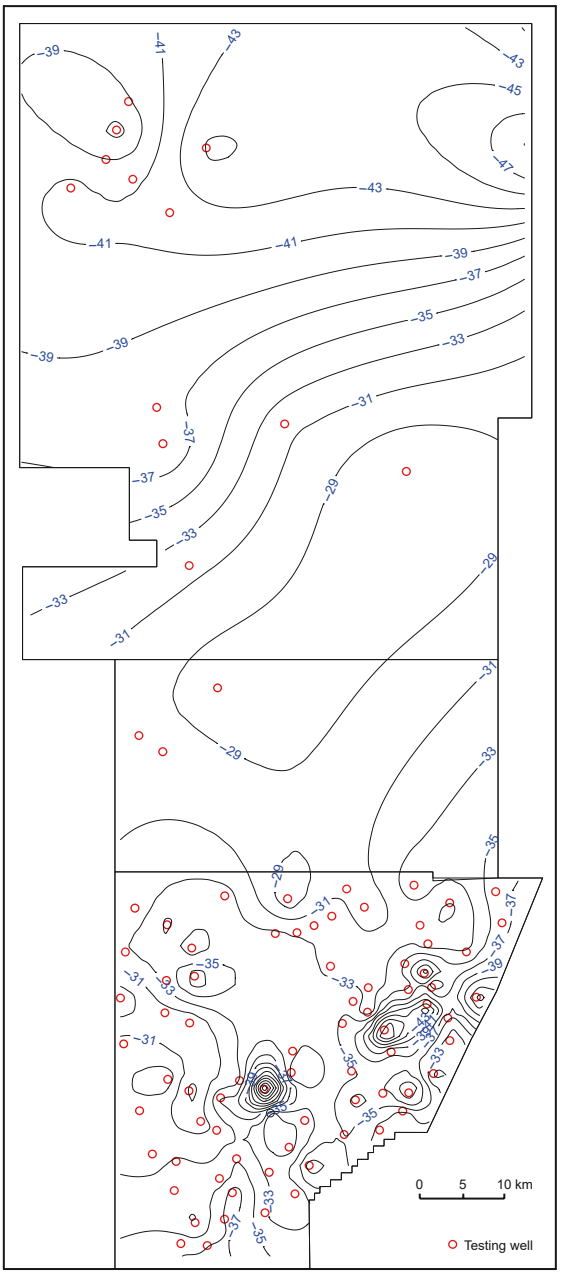

Fig. 16. Contour map of methane carbon isotopes in No.3 coal in the southwestern Qinshui Basin.

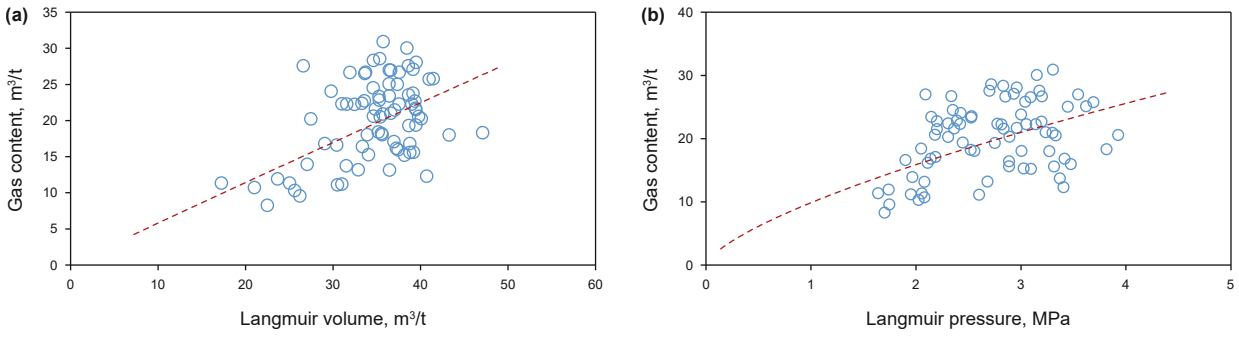

Fig. 15. Relationship between the coal seam gas content and Langmuir volume and Langmuir pressure. **(a)** Langmuir volume. **(b)** Langmuir pressure.

(4) The $\delta^{13}C_1$ values in this research region show a two-stage evolution pattern with increasing R^o_{max}. There is an inflection point in the relationship between the $\delta^{13}C_1$ values and R^o_{max} in coal at about 3.0%. When R^o_{max} is below 3.0%, the $\delta^{13}C_1$ values in CBM are heavier with increasing R^o_{max}. When R^o_{max} is above or equal to 3.0%, the $\delta^{13}C_1$ values in CBM are lighter with increasing R^o_{max}, which is mainly affected by the fractionation effect of methane carbon isotopes in coal during thermal evolution.

① Methane carbon isotope fractionation in coal is influenced by the process of coalification. The main reason for this is the higher energy required in ^{13}C–^{13}C bond breaking compared to ^{12}C–^{12}C bonds, while the ^{12}C–^{13}C bond exhibits intermediate energy requirements. When R^o_{max} is less than 3.0%, the probability for methane production from ^{12}C-^{12}C bond breaking is greater compared to ^{13}C–^{13}C bonding at lower temperatures during coalification. When the formation temperature increases, the possibility of methane production increases due to the breaking of ^{12}C–^{13}C and ^{13}C–^{13}C bonds (Saghafi, 2017). Eventually, the $\delta^{13}C_1$ values get heavier with the increase in vitrinite reflectance. When R^o_{max} is above or equal to 3.0%, the ^{12}C–^{13}C bond and ^{13}C–^{13}C bond breaking enhance the probability of methane production. However, with the increase in temperature and pressure, the side chains and functional groups of the basic structural units for coal continue to break and fall off, leading to a large reduction in quantity. Consequently, the probability of generating methane also decreases, leading to lighter $\delta^{13}C_1$ values with the increase in vitrinite reflectance.

② The distribution characteristics of the $\delta^{13}C_1$ values in different coalification stages are also different. The $\delta^{13}C_1$ values of humic-type conventional natural gas in biogenic, thermogenic gas, and pyrolytic gas are −78‰ to −55‰, −55‰ to −35‰, and greater than −35‰, respectively. The types of coal reservoirs in this area are mostly lean coal, poor coal, and anthracite, with measured R^o_{max} ranging from 1.77% to 4.26% and averaging 3.38%. The CBM in the area is primarily divided into thermogenic gas and pyrolytic gas, which is consistent with thermogenic and pyrolytic $\delta^{13}C_1$ values from humic-type conventional natural gas. The $\delta^{13}C_1$ values of No. 3 coal seam not only are basically in agreement with the statistical pattern of the CBM stable carbon isotope composition and evolution in China, but also resemble those of thermogenic the $\delta^{13}C_1$ values from organic matter This similarity is primarily mainly affected by the fractionation effect of carbon isotopes in CBM during thermal evolution (Mastalerz et al., 2004, 2008). As can be seen from Fig. 17, there is a certain dispersion between $\delta^{13}C_1$ values and R^o_{max} in No.3 coal seam. This indicates that the formation of CBM in this region is determined by the fractionation effect of carbon isotopes during thermal evolution. Besides, the spatial variations in methane isotopic composition may also be controlled by the CBM desorption-diffusion-migration process and the hydrodynamics effect, which need to be further explored.

(5) Carbon isotopes correlate with the gas content in coal. Based on the test statistics of carbon isotopes and CBM content from the No.3 coal seam of the Shanxi formation, the results show that carbon isotopes are heavier with the increasing gas content of methane in coal. There is a logarithmic function between methane carbon isotopes in coal and gas content (Fig. 18), and the relationship is shown below:

$$C = 7.0135 \ln(Q) - 54.34 \quad (20)$$

where C is the methane carbon isotope value in coal, ‰, which is negative. The determination coefficient R^2 is 0.43 and the total number of statistics is 89.

The gas content in coal seams is primarily influenced by the gas generation conditions, gas storage conditions, and preservation conditions. These mainly include factors such as geological structures, the lithology of the roof and floor of the coal seam, coal rock and quality, the degree of coal metamorphism, burial depth, and hydrogeological conditions. A high gas content in coal seams indicates favorable basic geological conditions for the accumulation of CBM, namely “generation, storage, and preservation,” which also results in heavier carbon isotopes of methane in the coal. This phenomenon arises because the adsorption of methane within the micro-pores of the coal matrix is primarily facilitated by van der Waals forces. The molecular weight of $^{13}CH_4$ methane is greater than that of $^{12}CH_4$ methane, resulting in a stronger adsorption capacity of $^{13}CH_4$ methane to the coal compared to $^{12}CH_4$ methane. Consequently, during the desorption process of methane from the coal matrix, a fractionation of carbon isotopes with different molecular weights occurs. This phenomenon is manifested through statistical regularity, whereby $^{12}CH_4$ methane is preferentially desorbed from the coal matrix over $^{13}CH_4$ methane during the desorption process of CBM. As a result, $^{13}CH_4$ methane tends to remain in the coal seam to a greater extent, leading to an enrichment of heavier carbon isotopes in the coal. Conversely, during the diffusion and migration processes, the desorbed CBM becomes relatively enriched with $^{12}CH_4$ methane, causing the carbon isotopes of methane in the coal to become lighter (Qin et al., 1998, 2000).

From the above, it can be observed that in coal seams of roughly similar rank, the higher the methane content, the heavier the

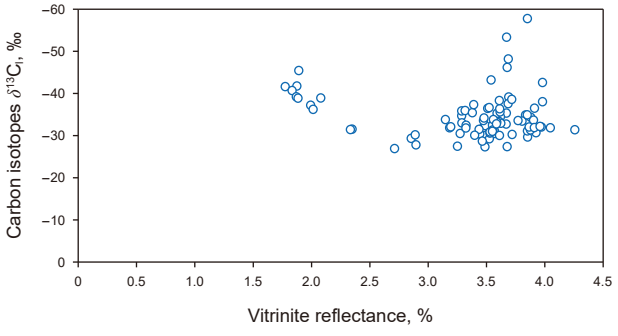

Fig. 17. Relationship between methane carbon isotopes and vitrinite reflectance in No.3 coal seam of the study area.

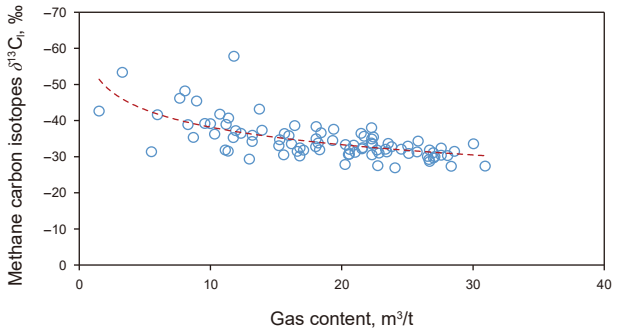

Fig. 18. Relationship between methane carbon isotopes and gas content in coal.

carbon isotopes of methane in the coal. This indicates favorable basic geological conditions for the accumulation of CBM, namely "generation, storage, and preservation," and also suggests a higher gas saturation. There is a strong correlation between the carbon isotope values of methane and the methane content in coal seams. These findings further demonstrate that the $\delta^{13}C_1$ characteristics of methane carbon isotopes in coal reflect the conditions for CBM accumulation and the magnitude of its gas content.

4. Conclusions

(1) V_L of air-dry basis, dry ash-free basis, and equilibrium moisture basis coal samples are 17.24–47.10 m^3/t, 25.83–54.43 m^3/t, and 14.79–40.74 m^3/t, respectively, and the corresponding average values are 34.60 m^3/t, 40.53 m^3/t, and 29.66 m^3/t. P_L ranges from 1.64 to 3.93 MPa, with an average value of 2.72 MPa. The distribution patterns of both V_L and P_L in the No. 3 coal seam of the study area are primarily controlled by coal composition and thermal maturity. The adsorption capacity of coal rises with mineral content and R^o_{max} in a logarithmic function. Besides, the adsorption capacity declines with increasing mineral content, moisture content, and ash yield in coal, which obeys a negative exponential function relationship.

(2) The methane content in No.3 coal seam is 8.28–30.92 m^3/t, with a mean value of 20.17 m^3/t. Methane content is primarily influenced by the burial depth, maceral composition, mineral content, moisture content, ash yield, coal metamorphic degree, and adsorption capacity of the coal. The gas content of the coal seam increases with greater burial depth and higher maceral composition content. In contrast, it decreases following a negative exponential function as the mineral content, moisture content, and ash yield of the coal increase. In addition, the gas content increases with increasing reflectivity in a logarithmic function rule. Moreover, with increasing Langmuir volume and pressure of the coal, the gas content increases by a power function rule.

(3) The $\delta^{13}C_l$ values of the No.3 coal seams in the naturally desorbed gas are between −26.95‰ and −57.80‰, with a mean value of −34.53‰. The $\delta^{13}C_1$ values in the study area show a two-stage variation pattern with increasing R^o_{max}. When R^o_{max} is below 3.0%, the $\delta^{13}C_1$ values of methane in coal become progressively heavier with increasing a R^o_{max}. When R^o_{max} reaches or exceeds 3.0%, the $\delta^{13}C_1$ values exhibit a lightning trend with further increases in R^o_{max}. This pattern is primarily controlled by carbon isotope fractionation effects during the thermal evolution of coal-derived methane.

CRediT authorship contribution statement

Ya Meng: Data curation, Funding acquisition, Conceptualization, Validation, Writing – original draft, Methodology, Formal analysis, Writing – review & editing. **Bin Zhang:** Resources, Writing – review & editing, Investigation. **Feng-peng Lai:** Conceptualization, Supervision.

Declaration of competing interest

No conflict of interest exits in the submission of this manuscript, and manuscript is approved by all authors for publication. I would like to declare on behalf of my co-authors that the work described was original research that has not been published previously, and not under consideration for publication elsewhere, in whole or in part.

Acknowledgements

This study was financially supported by the National Natural Science Foundation of China (No. 42372192), Shanxi Province science and technology plan joint unveiling project (No. 20201101002). The authors also thank the reviewers and editors for their constructive comments and suggestions on improving this manuscript.

References

Bao, Y., Wang, W.B., Ma, D.M., Shi, Q.M., Ali, A., Lv, D.K., Zhang, C.K., 2020. Gas origin and constraint of $\delta^{13}C(CH_4)$ distribution in the Dafosi mine field in the southern margin of the ordos basin, China. Energy Fuels 34 (11), 14065–14073. https://doi.org/10.1021/acs.energyfuels.0c02926.

Cao, L.T., Chang, S.L., Yao, Y.B., 2019. Application of seismic sedimentology in predicating sedimentary microfacies and coalbed methane gas content. J. Nat. Gas Sci. Eng. 69, 102944. https://doi.org/10.1016/j.jngse.2019.102944.

Cao, G.H., Zhang, H.X., Jiang, W.B., et al., 2019. A new gas-content-evaluation method for organic-rich shale using the fractionation of carbon isotopes of methane. SPE J. 24 (6), 2574–2589. https://doi.org/10.2118/197043-PA.

Chen, C.L., Lin, D.Y., 2005. Application of isothermal curves in estimating minable resource of CBM. J. China Inst. Min. Technol. 34 (5), 679–682. https://doi.org/10.1007/s11769-005-0036-4.

Chen, Z.H., Wang, Y.B., Song, Y., et al., 2008. Comparison of adsorption/desorption properties of CBM in different-rank coals. Nat. Gas. Ind. 28 (3), 30–32. https://doi.org/10.1016/S1876-3804(08)60015-4.

Esen, O., Ozer, S.C., Soylu, A., et al., 2020. Geological controls on gas content distribution of coal seams in the Kunuk coalfield, Soma Basin, Turkey. Int. J. Coal Geol. 231, 103602. https://doi.org/10.1016/j.coal.2020.103602.

Faiz, M.M., Aziz, N.I., Hutton, A.C., et al., 1992. Porosity and gas sorption capacity of some eastern Australian coals in relation to coal rank and composition. Coalbed methane symposium 4, 9–20.

Hou, J.S., Wang, Y., 1999. Interpretation of well logging data for CBM using bp neural network. Geology and Exploration 35 (3), 41–45.

Jiang, W.M., Liu, Q.M., Li, J.C., et al., 2024. Deciphering the origin and secondary alteration of deep natural gas in the Tarim basin through paired methane clumped isotopes. Mar. Petrol. Geol. 160, 106614. https://doi.org/10.1016/j.marpetgeo.2023.106614.

Li, G.H., Zhang, H., Cui, Y.J., et al., 2005. A predictive model of gas content in coal reservoirs based on multiple stepwise regression analysis: A case study from Qinshui Basin. Coal Geol. Explor. 33 (3), 22–25 (in Chinese).

Li, W.Z., Yong, H., Li, G.Z., 2010. Features and fractionation effect of methane isotope in CBM gas. Nat. Gas. Ind. 30 (11), 14–16 (in Chinese).

Li, G., Qin, Y., Yao, Z.L., et al., 2021. Differentiation of carbon isotope composition and stratabound mechanism of gas desorption in shallow-buried low-rank multiple coal seams: case study of well DE-A, northeast inner Mongolia. Nat. Resour. Res. 30, 1511–1526. https://doi.org/10.1007/s11053-020-09781-6.

Li, J.L., Ge, S.C., Liu, S., 2024. Differential adsorption of H_2S/CH_4 by bituminous coal and its competitive adsorption properties. Chem. Eng. J. 500, 157447. https://doi.org/10.1016/j.cej.2024.157447.

Lin, B.Q., Song, H.R., Zhao, Y., et al., 2019. Significance of gas flow in anisotropic coal seams to underground gas drainage. J. Petrol. Sci. Eng. 180, 808–819. https://doi.org/10.1016/j.petrol.2019.06.023.

Lin, H.F., Ji, P.F., Kong, X.G., et al., 2023. Experimental study on the influence of gas pressure on CH4 adsorption-desorption-seepage and deformation characteristics of coal in the whole process under triaxial stress. Fuel 333, 126513. https://doi.org/10.1016/j.fuel.2022.126513.

Liu, B., Chang, S.L., Zhang, S., et al., 2022. Coalbed methane gas content and its geological controls: research based on seismic-geological integrated method. J. Nat. Gas Sci. Eng. 101, 104510. https://doi.org/10.1016/j.jngse.2022.104510.

Ma, D.M., Zhang, S.A., Lin, Y.B., 2011. Isothermal adsorption and desorption experiment of coal and experimental results accuracy fitting. J. China Coal Soc. 36 (3), 477–480. https://doi.org/10.1007/s12182-011-0118-0.

Martin, S., 1980. The hydrogen and carbon isotopic composition of methane from natural gases of various origins. Geochem. Cosmochim. Acta 44, 649–661.

Mastalerz, M., Gluskoter, H., Rupp, J., 2004. Carbon dioxide and methane sorption in high volatile bituminous coals from Indiana, USA. Int. J. Coal Geol. 60 (1), 43–55. https://doi.org/10.1016/j.coal.2004.04.001.

Mastalerz, M., Drobniak, A., Strapoc, D., et al., 2008. Variations in pore characteristics in high volatile bituminous coals: implications for coal bed gas content. Int. J. Coal Geol. 76 (3), 205–216. https://doi.org/10.1016/j.coal.2008.07.006.

Meng, Y., Li, Z.P., 2018. Experimental comparisons of gas adsorption, sorption induced strain, diffusivity and permeability for low and high rank coals. Fuel 234, 914–923. https://doi.org/10.1016/j.fuel.2018.07.141.

Meng, Z.P., Guo, Y.S., Zhang, J.X., 2014. Application and prediction model of CBM content based on logging parameters. Coal Sci. Technol. 42 (6), 25–30.

Meng, Z.P., Liu, S.S., Li, G.Q., 2016. Adsorption capacity, adsorption potential and surface free energy of different structure high rank coals. J. Petrol. Sci. Eng. 146, 856–865. https://doi.org/10.1016/j.petrol.2016.07.026.
Meng, Z.P., Yan, J.W., Li, G.Q., 2017. Controls on gas content and carbon isotopic abundance of methane in qinnan-east coal bed methane block, Qinshui Basin, China. Energy Fuels 31 (2), 1502–1511. https://doi.org/10.1021/acs.energyfuels.6b03172.
Ni, Y.Y., Zhang, J.C., Yao, L.M., et al., 2024. Application of carbon and hydrogen isotopes in the natural gas origin study. Nat. Gas Geosci. 35 (11), 1897–1909. https://doi.org/10.1016/j.jnggs.2025.02.001.
Pan, J.N., Lv, M.M., Hou, Q.L., et al., 2019. Coal microcrystalline structural changes related to methane adsorption/desorption. Fuel 239, 13–23. https://doi.org/10.1016/j.fuel.2018.10.155.
Qin, Y., Tang, X.Y., Ye, J.P., 1998. Stable carbon isotope composition and desorption-diffusion effect of the upper paleozoic coalbed methane in north China. Geol. J. China Univ. 4 (2), 127–132.
Qin, Y., Tang, X.Y., Ye, J.P., et al., 2000. Characteristics and origins of stable carbon isotope in coalbed methane of China. J. China Inst. Min. Technol. 29 (2), 113–119.
Rice, D.D., 1993. Composition and origins of coalbed gas. AAPG (Am. Assoc. Pet. Geol.) Bull. 38 (1), 159–184.
Saghafi, A., 2017. Discussion on determination of gas content of coal and uncertainties of measurement. Int. J. Min. Sci. Technol. 27 (5), 741–748. https://doi.org/10.1016/j.ijmst.2017.07.024.
Skoczylas, N., Dutka, B., Sobczyk, J., 2014. Mechanical and gaseous properties of coal briquettes in terms of outburst risk. Fuel 134, 45–52. https://doi.org/10.1016/j.fuel.2014.05.037.
Su, X.B., Zhang, L.P., Lin, X.Y., 2005. Influence of coal rank on coal and sorption capacity. Nat. Gas. Ind. 25 (1), 19–21.
Tao, M.X., Chen, X.R., Li, Z.P., et al., 2021. Variation characteristic and mechanism of carbon isotope composition of coalbed methane under different conditions and its tracing significance. Fuel 302, 121039. https://doi.org/10.1016/j.fuel.2021.121039.
Wang, H.T., Xian, X.F., Du, Y.G., et al., 2002. Analytic method of calculating gas content in coal seams in deep mining. J. China Inst. Min. Technol. 31 (4), 367–369.
Xu, S.P., Hu, E.R., Li, X.C., et al., 2021. Quantitative analysis of pore structure and its impact on methane adsorption capacity of coal. Nat. Resour. Res. 30, 605–620. https://doi.org/10.1007/s11053-020-09723-2.
Ye, X., Liu, H.L., 2008. Difference of desorption mechanism in CBM with high and low coal ranks. Natural Gas Technology and Economy 2 (2), 19–22.
Zhang, J.B., Tao, M.X., 2000. Geological significances of CBM carbon isotope in CBM exploration. Acta Sedimentol. Sin. 8 (4), 611–614.
Zhang, T.J., Xu, H.J., Li, S.G., et al., 2009. The effect of temperature on the adsorbing capability of coal. J. China Coal Soc. 34 (6), 802–805.
Zhang, J.Y., Liu, D.M., Cai, Y.D., et al., 2018. Carbon isotopic characteristics of CH_4 and its significance to the gas performance of coal reservoirs in the Zhengzhuang area, Southern Qinshui Basin, North China. J. Nat. Gas Sci. Eng. 58, 135–151. https://doi.org/10.1016/j.jngse.2018.08.009.
Zhang, K., Meng, Z.P., Wang, X.M., 2019. Distribution of methane carbon isotope and its significance on CBM accumulation of No.2 coal seam in Yanchuannan CBM block, Ordos Basin, China. J. Petrol. Sci. Eng. 174, 92–105. https://doi.org/10.1016/j.petrol.2018.11.013.
Zhang, S., Zhang, X.D., Li, G.Z., et al., 2019. Distribution characteristics and geochemistry mechanisms of carbon isotope of coalbed methane in central-southern Qinshui Basin, China. Fuel 244, 1–12. https://doi.org/10.1016/j.fuel.2019.01.129.
Zhang, H., Cai, X.L., Ni, P., et al., 2025. Prediction of coalbed methane content based on composite logging parameters and PCA-BP neural network. J. Appl. Geophys. 236, 105681. https://doi.org/10.1016/j.jappgeo.2025.105681.
Zhou, W., Gao, K., Xue, S., et al., 2020. Experimental study of the effects of gas adsorption on the mechanical properties of coal. Fuel 281, 118745. https://doi.org/10.1016/j.fuel.2020.118745.